Acta Oceanol. Sin., 2020, Vol. 39, No. 10, P. 81–95
https://doi.org/10.1007/s13131-020-1663-4
http://www.hyxb.org.cn
E-mail: hyxbe@263.net

Geological characteristics of the Nankai Trough subduction zone and their tectonic significances

Jie Zhang[1, 3], Ling Chen[1, 2*], Zihua Cheng[4], Limei Tang[1]

[1] Key Laboratory of Submarine Geosciences, Ministry of Natural Resources/Second Institute of Oceanography, Ministry of Natural Resources, Hangzhou 310012, China

[2] Key Laboratory of Marine Mineral Resources, Guangzhou Marine Geological Survey, Ministry of Natural Resources, Guangzhou 510760, China

[3] Southern Marine Science and Engineering Guangdong Laboratory (Zhuhai), Zhuhai 519080, China

[4] Key Laboratory of Ocean and Marginal Sea Geology, South China Sea Institute of Oceanology, Chinese Academy of Sciences, Guangzhou 510301, China

Received 6 January 2020; accepted 27 March 2020

Abstract

The Nankai Trough subduction zone is a typical subduction system characterized by subduction of multiple geological units of the Philippine Sea Plate (the Kyushu-Palau Ridge, the Shikoku Basin, the Kinan Seamount Chain, and the Izu-Bonin Arc) beneath the Eurasian Plate in the southwest of Japan. This study presents a geophysical and geochemical analysis of the Nankai Trough subduction zone in order to determine the features and subduction effects of each geological unit. The results show that the Nankai Trough is characterized by low-gravity anomalies (–20 mGal to –40 mGal) and high heat flow (60–200 mW/m^2) in the middle part and low heat flow (20–80 mW/m^2) in the western and eastern parts. The crust of the subducting plate is 5–20 km thick. The mantle composition of the subducting plate is progressively depleted from west to east. Subduction of aseismic ridges (e.g., the Kyushu-Palau Ridge, the Kinan Seamount Chain, and the Zenisu Ridge) is a common process that leads to a series of subduction effects at the Nankai Trough. Firstly, aseismic ridge or seamount chain subduction may deform the overriding plate, resulting in irregular concave topography along the front edge of the accretionary wedge. Secondly, it may have served as a seismic barrier inhibiting rupture propagation in the 1944 M_w 8.1 and 1946 M_w 8.3 earthquakes. In addition, subduction of the Kyushu-Palau Ridge and hot and young Shikoku Basin lithosphere may induce slab melting, resulting in adakitic magmatism and the provision of ore-forming metals for the formation of porphyry copper and gold deposits in the overriding Japan Arc. Based on comparisons of their geophysical and geochemical characteristics, we suggest that, although the Izu-Bonin Arc has already collided with the Japan Arc, the Kyushu-Palau Ridge, which represents a remnant arc of the Izu-Bonin Arc, is still at the subduction stage characterized by a single-vergence system and a topographic boundary with the Japan Arc.

Key words: Nankai Trough, subduction zone, velocity structure, gravity modeling, geochemistry, petrology, slab melting, geological effect

Citation: Zhang Jie, Chen Ling, Cheng Zihua, Tang Limei. 2020. Geological characteristics of the Nankai Trough subduction zone and their tectonic significances. Acta Oceanologica Sinica, 39(10): 81–95, doi: 10.1007/s13131-020-1663-4

1 Introduction

Subduction zones are one of the most active and complex regions in the world (e.g., Zang and Ning, 2002; Idini et al., 2017), which evolve differently from collision zones (e.g., Pusok et al., 2018). Several studies on the characteristics of subduction- and collision-related zones (e.g., topography, lithospheric deformation, magmatism) have been conducted (e.g., Tang et al., 2011; Wu et al., 2016), allowing scientists to divide the formation of a subduction-collision phase into three stages: subduction, transition from subduction to collision, and continental (arc) collision (e.g., Beaumont et al., 1996; Soh et al., 1998; Saito and Tani, 2017).

The Nankai Trough is a typical subduction system located at the southwest of the Japan Arc. The Kyusyu-Palau Ridge (KPR) and the Izu-Bonin Arc (IBA) separate the Nankai Trough from other subduction zones. The Philippine Sea Plate (PSP) is subducting along the Nankai Trough at a rate of approximately 50 mm/a in the west to less than 30 mm/a in the east (Heki and Miyazaki, 2001). Soh et al. (1998) proposed that subduction of the PSP at the eastern end of the Nankai Trough resulted in collision of the IBA with the Honshu Arc in central Japan, forming an Izu collision zone. However, the current subduction stage of the KPR,

Foundation item: The Open Research Fund of the Key Laboratory of Marine Mineral Resources, Guangzhou Marine Geological Survey, MNR under contract No. KLMMR-2017-B-01; the National Program on Global Change and Air–Sea Interaction, SOA under contract No. GASI-GEOGE-01; the Scientific Research Fund of the Second Institute of Oceanography, MNR under contract Nos JG1903 and QNYC1901; the National Natural Science Foundation of China under contract Nos 41706044, 41706041, 41890811 and 91858214; the Open Research Fund of the Key Laboratory of Ocean and Marginal Sea Geology, Chinese Academy of Sciences under contract No. OMG2019-04.

*Corresponding author, E-mail: chenling@sio.org.cn

a remnant arc of the proto-IBA, is still under debate. Yan and Shi (2011) and Tang et al. (2011) suggested that the KPR at the western end of the Nankai Trough subducted beneath the Kyushu Arc. Cao et al. (2014) mentioned that subduction in the southwestern part of Japan was characterized by collision between the KPR and the Kyushu Arc. Furthermore, the formation of felsic tonalite (Haraguchi et al., 2003) and a thick crust with a granitic material layer (Li, 1997) in the northern KPR may be related to continental crust accretion associated with collision (Haraguchi et al., 2003).

In addition to the KPR and the IBA, several geological units are also identified along the Nankai Trough. In the eastern part, there is a basement high identified as the Zenisu Ridge, which is subducting below the trough. Meanwhile, the Kinan Seamount Chain (KSC) and the Shikoku Basin are subducting beneath the middle part of the trough (e.g., Kobayashi et al., 1995). Previous geophysical and geochemical studies have suggested that subduction processes, especially those related to aseismic ridge (seamount chain) subduction, are key factors controlling crustal deformation (e.g., Park et al., 2009), large inter-plate earthquakes (e.g., Kodaira et al., 2002, 2004; Liu and Zhao, 2014; Niu et al., 2020), and magmatism (e.g., Cao et al., 2014; Morris, 1995; Shibata et al., 2014). However, there have been few comprehensive summaries of these studies. Therefore, this study integrates previous geochemical and geophysical data to clarify the characteristics of the Nankai Trough. Two key issues are discussed: (1) the subduction stage of the KPR and (2) the effects of aseismic ridge (seamount chain) subduction.

2 Geological setting

The PSP is a narrow NS-trending rhombic-shaped plate, surrounded by several convergent plate boundaries (Fig. 1). The western and southwestern parts of the PSP are bound by the Izu-Bonin Trench, the Nankai Trough, and the Philippine Trench. In the eastern part, the Izu-Bonin Trench and Mariana Trench are regarded as plate boundaries (Zhang et al., 2012; Chen et al., 2014). The Yap Trench and the Palau Trench define the southern boundary of the PSP. Along the Nankai Trough, the subducting PSP is composed of several geological units, including the KPR, the Shikoku Basin, the KSC, the Zenisu Ridge, and the IBA (Kobayashi et al., 1995). The KPR is a discontinuous ridge (Tang et al., 2011) located in the middle of the Philippine Sea. Generally, the ridge lies 2 000–3 000 m above the floor of the basin and extends continuously over a distance of 2 600 km from off Kyushu Island in the north toward Palau Island in the south (Ishizuka et al., 2011). The KPR is a remnant arc of the proto-IBA, which was split during the period from 30 Ma to 15 Ma (Okino et al., 1994). The northern end of the KPR is 100–150 km wide and extends NNW (Ishizuka et al., 2011). According to $^{36}Ar/^{40}Ar$ and $^{40}Ar/^{39}Ar$ dating of lavas collected from the Ocean Drilling Program Hole 786 of the proto-IBA, their ages are 47–45 Ma (Cosca et al., 1998). Combined K-Ar and $^{40}Ar/^{39}Ar$ dating data indicate that boninite-series magmatism in the Izu-Bonin forearc (and remnant arc at Palau) continued until approximately 35 Ma (Cosca et al., 1998). The Shikoku Basin was formed by back-arc opening between the KPR and the IBA. From 26 Ma to 15 Ma, NNW-SSE seafloor spreading first developed, then continued in a NE-SW direction in the final stages (Okino et al., 1999). The KSC is the product of post-spreading magmatism generated along the fossil spreading ridge of the Shikoku Basin, with an age ranging from 15.7 Ma to 9.6 Ma (Okino et al., 1999; Ishizuka et al., 2009). The Zenisu Ridge is a conspicuous topographic high rising 2 000 m from the bottom of the Nankai Trough (Nakanishi et al., 1998).

3 Data

3.1 *Geological data*

The free-air gravity anomaly data (S&S V24.1) used in this study were obtained from the University of California, San Diego, and the Scripps Institute of Oceanography, with a grid spacing of 1′ × 1′ (Sandwell and Smith, 2009; Sandwell et al., 2014). Magnetic anomaly data were derived from the geomagnetic intensity anomaly database (EMAG2) (Maus et al., 2009), with a measured height of 4 km and a grid spacing of 2′ × 2′. Heat flow data were derived from the International Heat Flow Committee database (Lee, 1964).

We collected data from five seismic refraction/refection survey profiles along the Nankai Trough subduction zone (Fig. 1) (Kodaira et al., 2002, 2004, 2005; Takahashi et al., 2002; Nakanishi et al., 2002; Nishizawa et al., 2009), which cover all subducting geological units of the Nankai Trough, including the KPR, the Shikoku Basin, the KSC, and the Zenisu Ridge. All seismic profiles were modeled based on global 1′ × 1′ gravity grid data (Sandwell and Smith, 2009; Sandwell et al., 2014) in order to clarify the density structures simultaneously. For the gravity modeling, we used a 2D algorithm by Talwani et al. (1959).

3.2 *Geochemical data*

Geochemical data used in this study were as follows: the major elements of mafic, intermediate, and felsic volcanic rocks from the PSP near the Nankai Trough; the rare earth element (REE) contents of basalt from the northern part of the KPR, the KSC, and the IBA; age data of plutonic rocks from the northern KPR and volcanic rocks from the northern part of the KSC and the IBA; and Pb isotopic data of volcanic rocks from the Japan Arc and basalts from the northern part of the KPR, the KSC, and the IBA. Data of volcanic rocks in the Japan Arc and plutonic rocks in the northern KPR were derived from Shibata et al. (2014) and Haraguchi et al. (2003), respectively. Other data were derived from the PetDB database (http://www.earthchem.org/petdb). Rock sample stations are shown in Fig. 1 and detailed rock data source are presented in the captions of the geochemical figures.

4 Characteristics of the Nankai Trough

4.1 *Geophysical characteristics*

4.1.1 *Gravity anomaly, magnetic anomaly, and heat flow of the Nankai Trough*

Positive anomalies are observed over the KPR, the Shikoku Basin, the KSC, and the IBA (Fig. 2a). In terms of the amplitude, the values of the gravity anomaly vary significantly in the transition zone from the PSP to the Nankai Trough, revealing a low-gravity anomaly zone. Gravity anomalies of the Nankai Trough and the forearc basin (excluding the forearc area in Kyushu Island) are relatively low, with values concentrated in the range of –20 mGal to –40 mGal. The free-air gravity anomalies measured in the forearc area on Kyushu Island are lower than those of other forearc areas, and gravity anomaly values are concentrated in the range of –40 mGal to 130 mGal. Variations in the free-air gravity anomalies may reflect different densities resulting from the subducting material (Chen et al., 2014). The density of the upper crust is generally light, which corresponds to a low-air gravity anomaly. We propose that negative gravity anomalies in the Kyushu region of the western Nankai Trough may be related to the thick sediments and upper crust above the subduction zone.

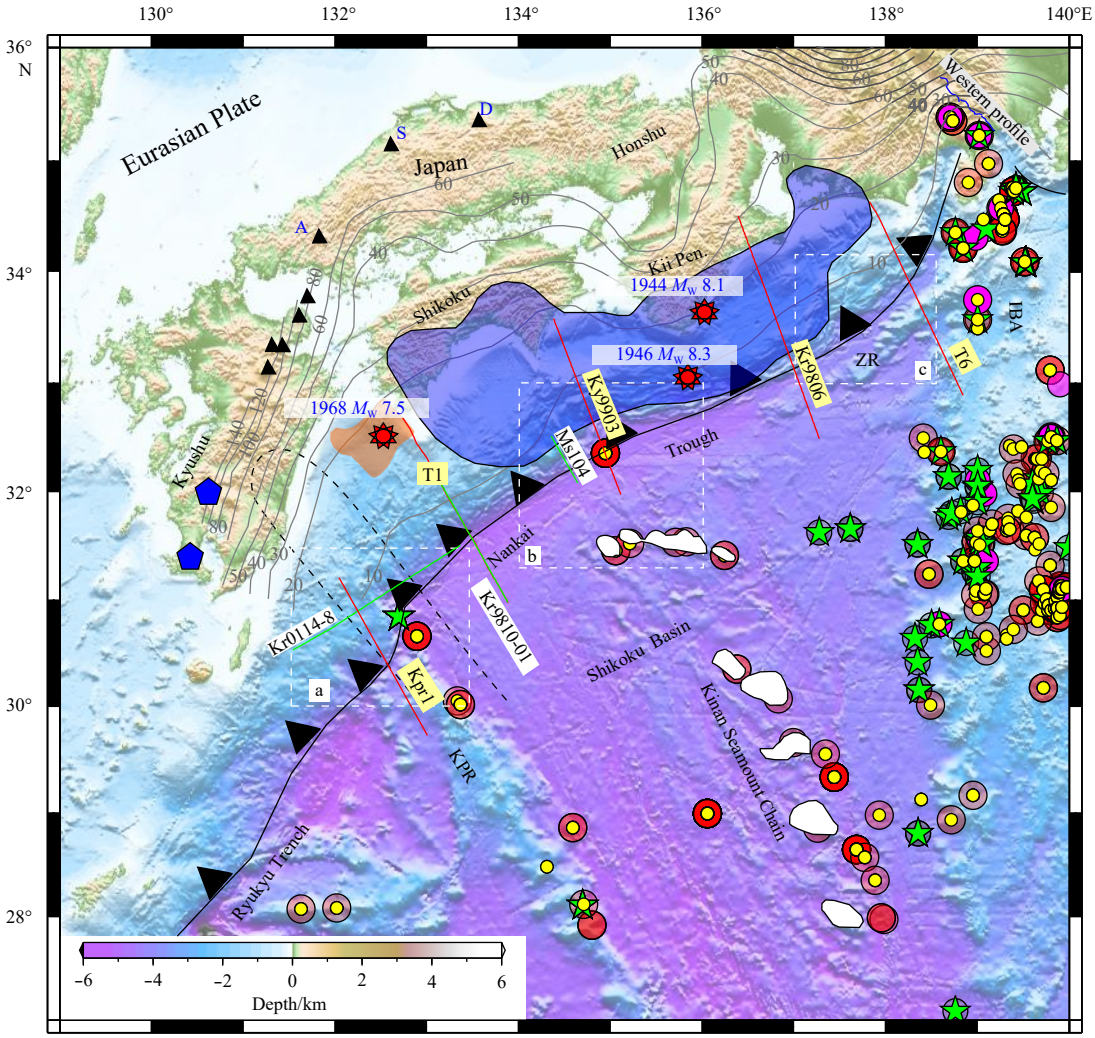

Fig. 1. Bathymetric map of the Philippine Sea Plate (GEBCO Compilation Group, 2020). Red (blue) and green lines show the ocean-bottom seismometer (OBS) (Kodaira et al., 2002, 2004, 2005; Takahashi et al., 2002; Nakanishi et al., 2002; Nishizawa et al., 2009) and multiple channel seismic lines (Park et al., 2002, 2009), respectively. Red, yellow, and pink circles represent mafic rock, basalt, and felsic rock stations, respectively. Green stars denote intermediate rock stations. Black triangles indicate volcanos with adakite eruptions and the volcanos labelled as D (Daisen), S (Sambe), and A (Aonoyama) correspond to the leading edge of the subducted Shikoku Basin (Morris, 1995; Shibata et al., 2014). Blue polygons denote low-sulfidation epithermal gold deposits (Hishikari) and high-sulfidation gold deposits (Nansatsu) (Cooke et al., 2005). Orange and blue shaded areas show the rupture zones of the 1968 Hyuga earthquake (red polygon, M_w=7.5) (Park et al., 2009; Yagi et al., 1998), the 1944 earthquake (red polygon, M_w=8.1), and the 1946 earthquake (red polygon, M_w=8.3) (Sagiya and Thatcher, 1999), respectively. The black solid line with triangles indicates the subduction zone. The black dotted line marks the inferred Kyushu-Palau Ridge beneath the toe of the forearc accretionary wedge (Park et al., 2009). Gray lines outline the depth contours of the upper surface of the PSP (Zhao et al., 2012). White shaded areas indicate the Kinan Seamount Chain. The white dashed-line boxes outline the boundaries of Fig. 9. KPR: Kyushu-Palau Ridge, ZR: Zenisu Ridge, IBA: Izu-Bonin Arc. Rock data are derived from the PetDB database (http://www.earthchem.org/petdb).

A series of magnetic lineations are observed at the Philippine Sea Basin near the Nankai Trough, which is indicative of a typical oceanic basin (Fig. 2b). However, these magnetic lineations are untraceable at the Nankai Trough, resulting in different magnetic anomaly characteristics between the Japan Arc and the oceanic basin. The magnetic anomalies at the Nankai Trough have amplitudes of –80 nT to 160 nT. The most striking feature of the magnetic anomaly map is the existence of dipolar anomalies associated with basement highs on the PSP, such as the KPR (Nishizawa et al., 2017).

Figure 2c shows that the heat flow in the middle part of the trough is relatively high (60–200 mW/m^2), and lower in the western and eastern parts (20–80 mW/m^2). The high heat flow values in the middle part of the trough may be related to subduction of the oceanic crust of the young Shikoku Basin, whereas the low heat flow may be due to subduction of the relatively older KPR and Zenisu Ridge (Xu et al., 2003; Chen et al., 2014). With respect to the island arc area, the highest heat flow values were measured in the Kyushu Island, especially for the southwestern part of the island, with values of 1 000–4 000 mW/m^2, whereas low heat flow values of 30–100 mW/m^2 were measured in the Shikoku Peninsula, Kii Peninsula, and Honshu Island.

4.1.2 *Structural characteristics of the Nankai Trough subduction zone*

Figure 3 shows the velocity structures of the shallow crust

across the Nankai Trough subduction zone. For this research, all five seismic profiles were modeled based on free-air gravity anomaly data (Fig. 4) in order to simultaneously clarify the density structures of the Nankai Trough subduction zone. Profiles Ky9903 and T6, shown in Fig. 3, consist of sections recorded by both ocean-bottom seismometers (OBSs) and land stations. We

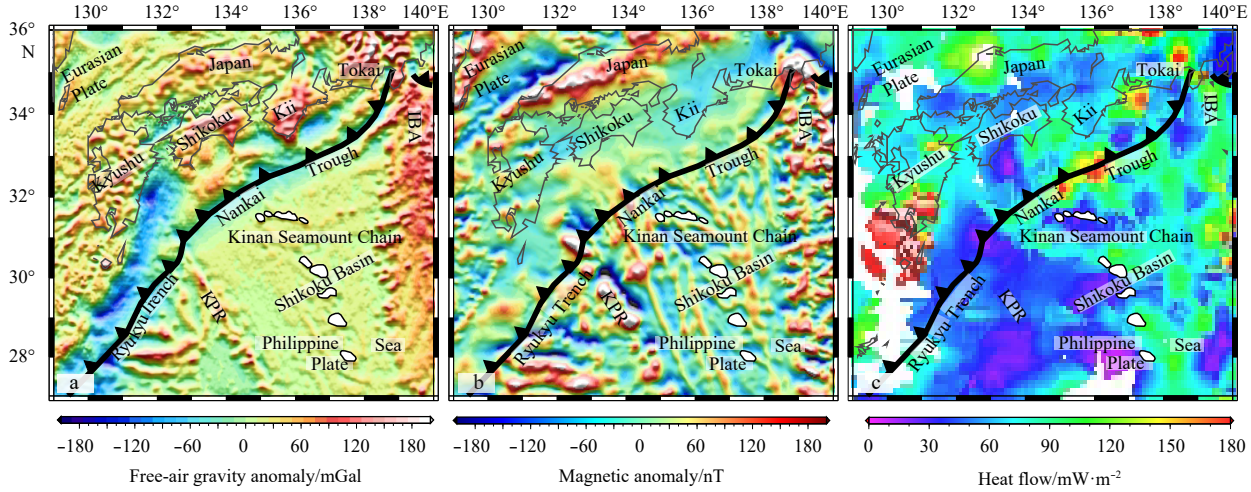

Fig. 2. Maps of the study area. a. Free-air gravity anomaly map of the study area. S&S V24.1 data (Sandwell and Smith, 2009; Sandwell et al., 2014) are derived from the University of California, San Diego and the Scripps Institute of Oceanography, with a grid spacing of 1′×1′. b. Magnetic anomaly map of the study area. Data are derived from the total geomagnetic intensity anomaly database EMAG2 (Maus et al., 2009). The measured height is 4 km and the grid spacing is 2′×2′. c. Heat flow map of the study area. Data are derived from the International Heat Flow Committee database (Lee, 1964). The grey curves outline the coastline and all other annotations are the same as those in Fig. 1.

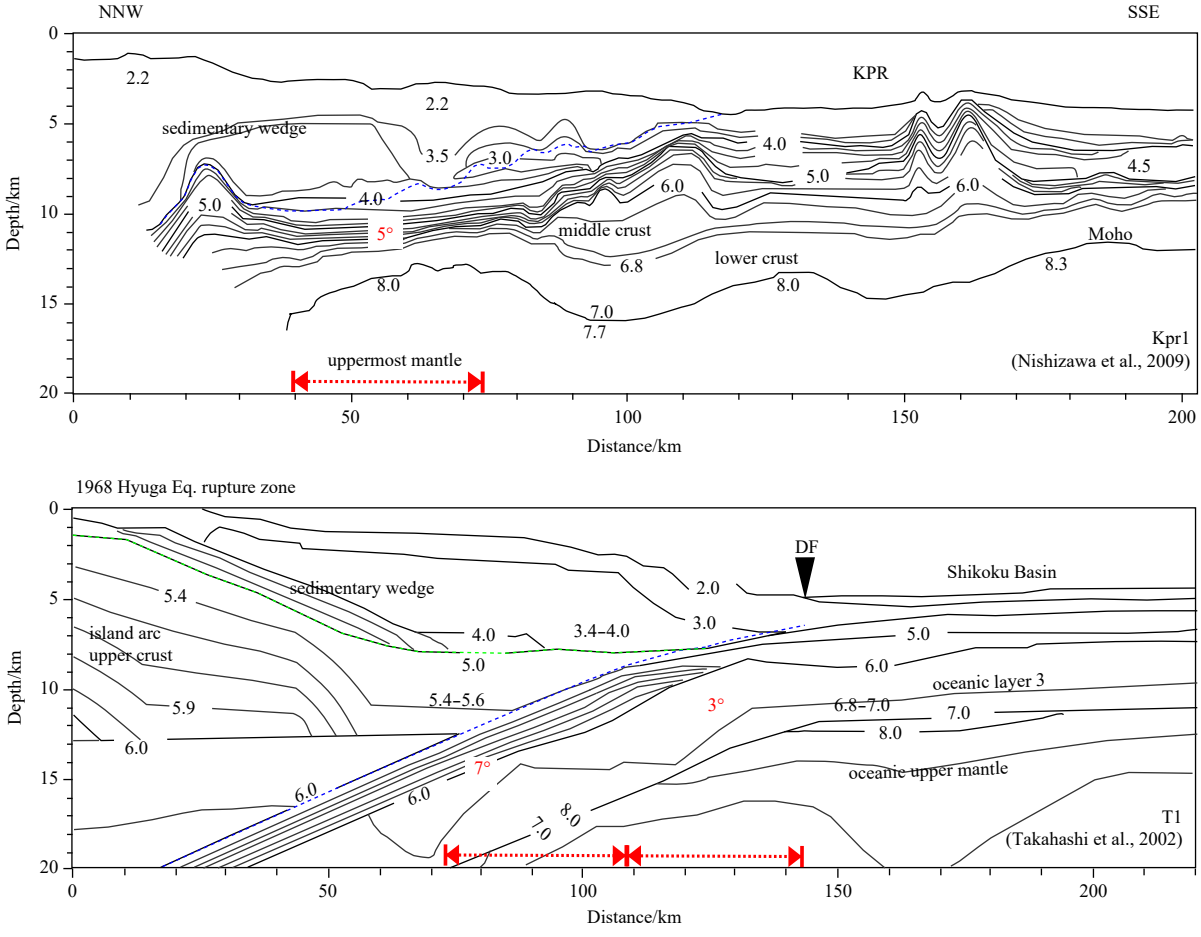

Fig. 3.

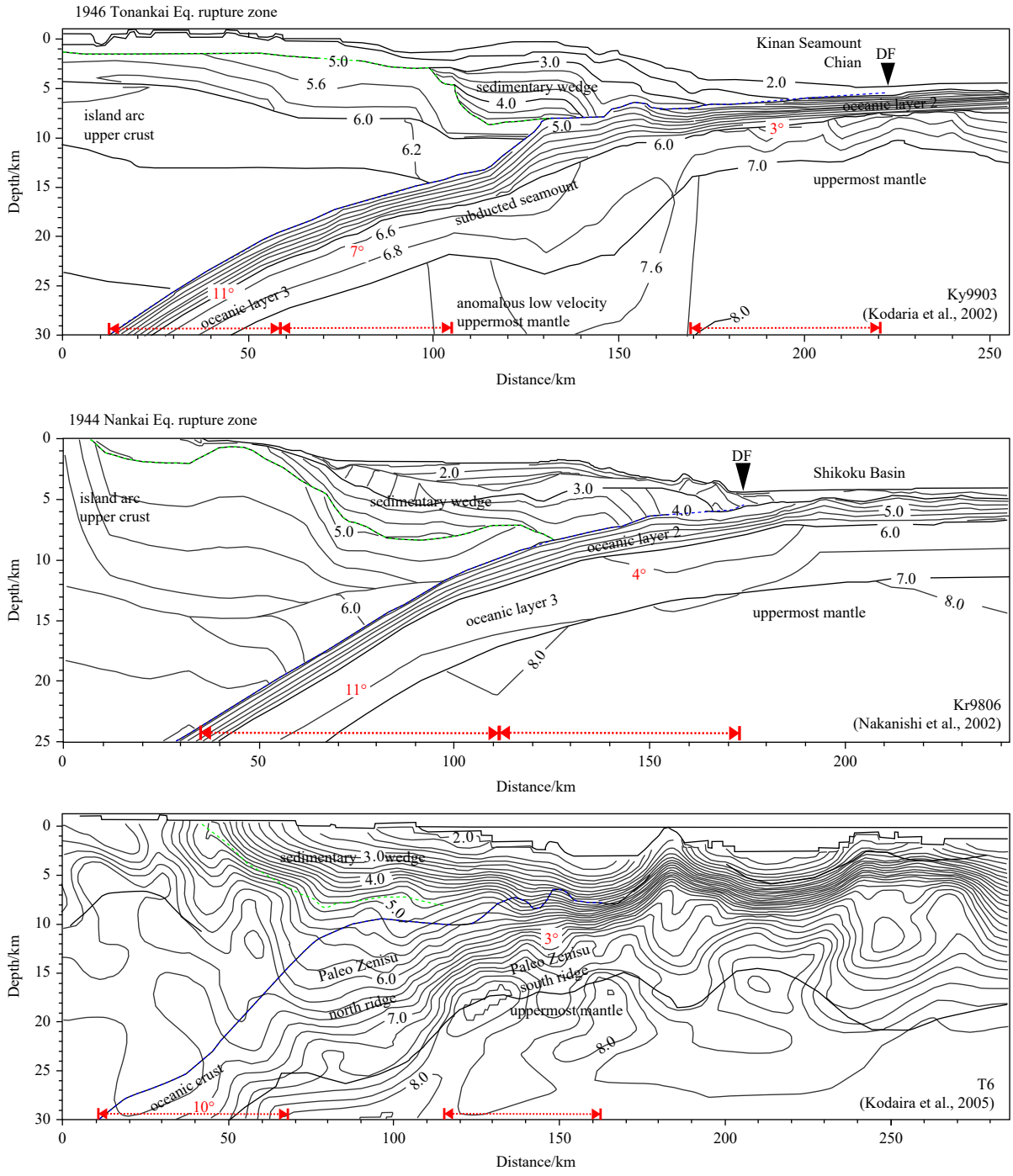

Fig. 3. Velocity characteristics of the Nankai Trough subduction zone (modified after Kodaira et al., 2002, 2005; Takahashi et al., 2002; Nakanishi et al., 2002; Nishizawa et al., 2009). The location of the profiles is shown in Fig. 1. The green dashed line marks the boundary between the sedimentary wedge and the upper crust of the island arc. The blue dashed line indicates the presumed plate boundary, whereas the solid part represents the width of the oceanic crust and the sedimentary wedge contact zone. The deformation front (DF) along T1, Kr9704, Ky9903, and Kr9806 is plotted based on multiple studies (Park et al., 2002; Nakanishi et al., 2002; Kodaira et al., 2000, 2002). The co-seismic rupture zone of the 1944 event (blue bar) (Sagiya and Thatcher, 1999) is shown above the crustal model of Kr9704 and KY9903. Co-seismic rupture zones of the 1946 (blue bar) (Sagiya and Thatcher, 1999) and 1968 events (orange bar) (Yagi et al., 1998) are shown above the crustal models of Kr9806 and T1, respectively. Red numbers with units of degrees denote the subduction angle of the crust. KPR: Kyushu-Palau Ridge, IBA: Izu-Bonin Arc.

modeled the sections recorded by OBSs only; hence, the length of profiles Ky9903 and T6 were shortened in the gravity modeling (Fig. 4). Nakanishi et al. (2002) suggested that the Nankai Trough subduction zone consists of a sedimentary wedge, subducted plate, and island arc crust. All profiles recorded portions of these three features, except for the Kpr1 profile, which did not record the upper crust of the island arc due to the loci (Fig. 1).

As shown in Figs 3 and 4 and Table 1, a sedimentary wedge

occurs beneath the slope, with velocities (V_p) of less than 5 km/s and densities (ρ) ranging from 2.2 cm/g³ to 2.6 cm/g³, which is interpreted as a Neogene-Quaternary accretionary prism (Kodaira et al., 2004, 2005). This sedimentary wedge is characterized by significant thickening to the north. At the region where the sedimentary wedge meets the edge of the subducted plate, the young

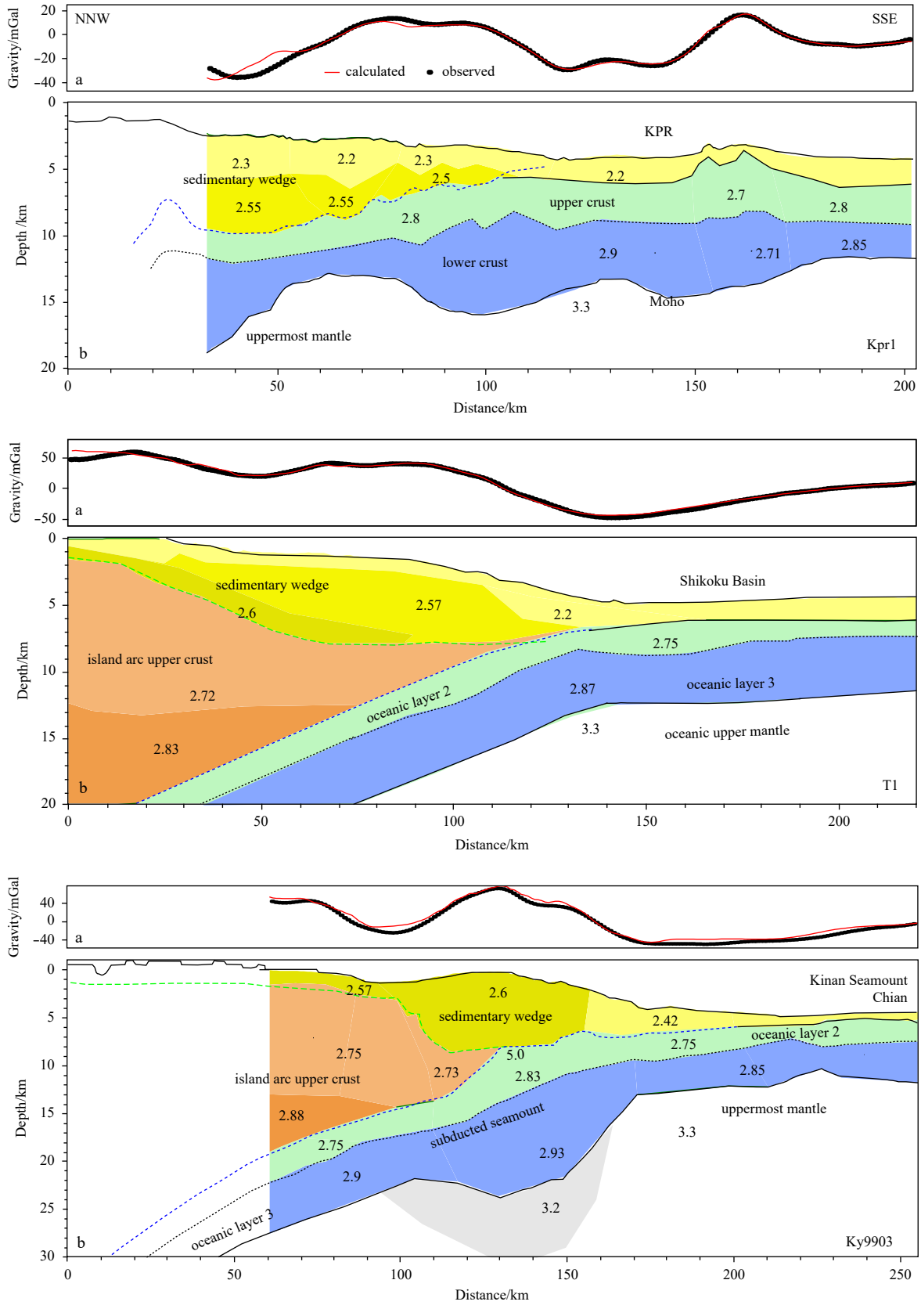

Fig. 4.

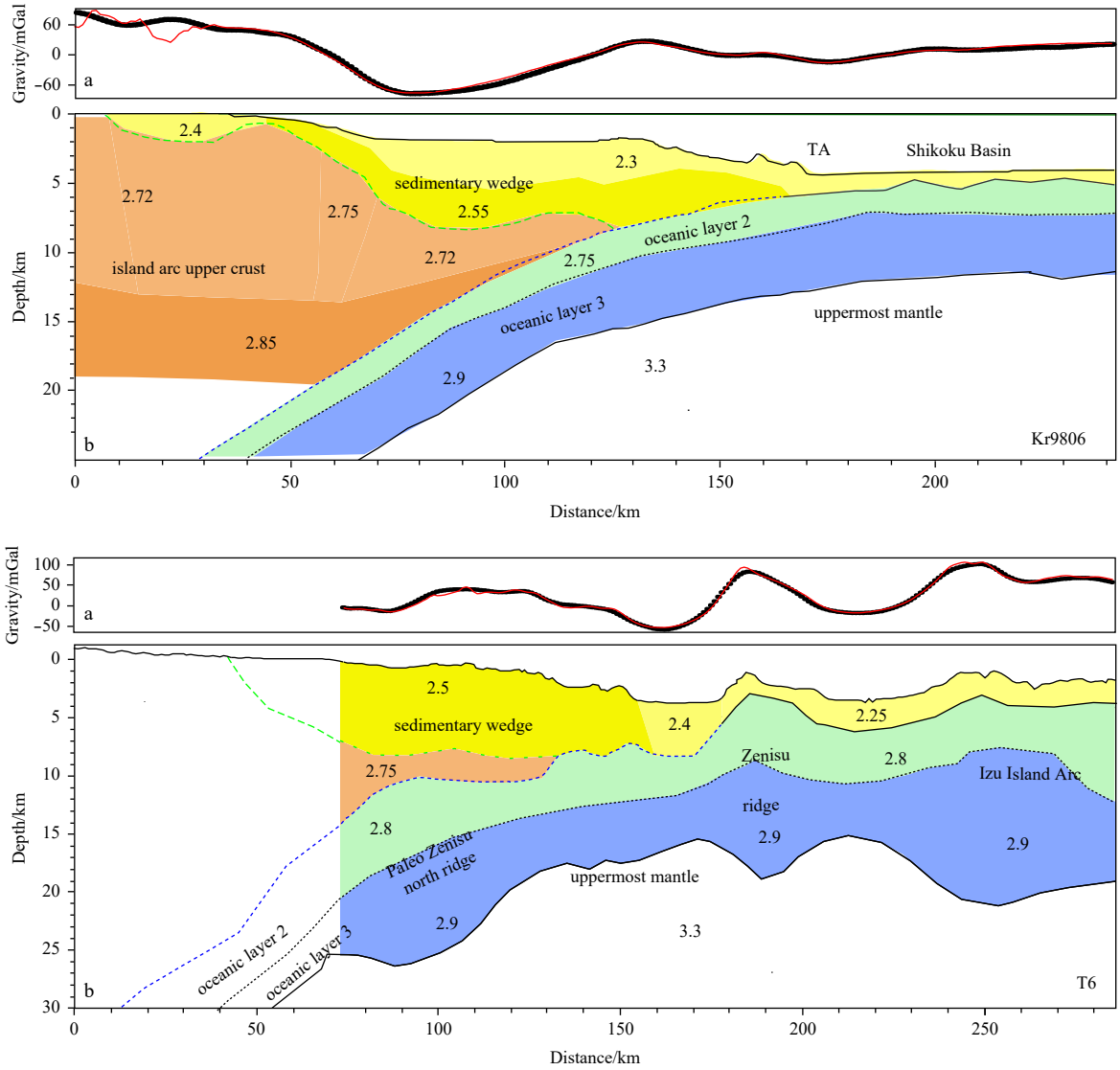

Fig. 4. Density characteristics of the Nankai Trough subduction zone. a. Observed and calculated gravity values for Profiles Kpr1, T1, Ky9903, Kr9806, and T6. Dotted lines represent the observed free-air gravity anomalies and solid lines are the gravity anomalies calculated using the density model. b. Preferred gravity models. The location of the profile is shown in Fig. 1. The green dashed line marks the boundary between the sedimentary wedge and the upper crust of the island arc, and the blue dashed line indicates the presumed plate boundary. The final RMS values are 3.2 mGal, 3.4 mGal, 7.7 mGal, 8.7 mGal, and 4.8 mGal for Profiles Kpr1, T1, Ky9903, Kr9806, and T6, respectively. KPR: Kyushu-Palau Ridge, IBA: Izu-Bonin Arc.

Table 1. Structural characteristics of the Nankai Trough subduction zone

Profile		Kpr1	T1	Kr9806	Ky9903	T6
Seismic velocity of the subducted plate/km·s^{-1}		Kyushu–Palau Ridge (KPR) ~4.0–7.0	Shikoku Basin ~5–7.0	Shikoku Basin 4.5–6.9	Kinan Seamount Chain 4.6–7.0	Zenisu Ridge ~5.2–7.4
Density of the subducted plate/g·cm^{-3}	Upper crust	2.7–2.8	2.75	2.75	2.83	2.8
	Lower crust	2.9	2.87	2.90	2.93	2.9
Thickness of the subducted plate/km		~10	~5	~5	~6–14	~20
Velocity of upper crust of island arc/km·s^{-1}		unknown	>5	>5	>5	>5
Density of the upper crust of island arc/g·cm^{-3}		unknown	2.72–2.83	2.73–2.88	2.72–2.85	2.75
Velocity of the accretionary wedge/km·s^{-1}		3.2–3.3	3.4–4.0	1.6–4.7	2.0–4.2	2–5
Density of the accretionary wedge/g·cm^{-3}		2.2–2.55	2.2–2.6	2.42–2.6	2.3–2.55	2.25–2.5
Reference		Nishizawa et al. (2009)	Takahashi et al. (2002)	Nakanishi et al. (2002)	Kodaira et al. (2002)	Kodaira et al. (2004, 2005)

oceanic crust of the Shikoku Basin is ~5 km thick with V_p being 5–7 km/s and ρ being 2.75–2.90 g/cm^3. The crust of the KPR is up to 10 km thick with V_p being 4.0–7.0 km/s and ρ being ~2.7 g/cm^3. The crust of the KSC reaches a maximum thickness of 14 km and is characterized by velocities in the range of 4.6–7.0 km/s and densities in the range of 2.83–2.93 g/cm^3. The Zenisu Ridge, located on the western edge of the IBA, is up to 20 km thick (~150 km at Profile T6) with V_p being 5.4–7.4 km/s and ρ being 2.8–2.9 g/cm^3. These results demonstrate the diversity of velocity and density characteristics among the different geologic units, especially between the seamount chain (i.e., the ridge) and the normal oceanic crust.

4.2 *Geochemical characteristics*

In the vicinity of the Nankai Trough (130°–139°E) (Fig. 1), few basement rocks are exposed at the trench axis, where the KPR and the IBA intersect with the trough (Haraguchi et al., 2012; Kimura et al., 2010). The samples are predominantly mafic igneous rocks and a few intermediate rocks such as andesite (Fukuda et al., 2008; Ishizuka et al., 2009; Haraguchi et al., 2012). In the PSP, mafic rocks are widely exposed across the different geological units, including oceanic ridges, seamounts, and island arcs. Due to sediment coverage, basement rocks are rarely sampled in the deep basin. Intermediate volcanic rocks are mainly distributed across the IBA and the KPR (Haraguchi et al., 2012). Felsic rocks are largely absent from the Nankai Trough, the KSC, and the Shikoku Basin, with some plutonic tonalites in the northern tip of KPR (Haraguchi et al., 2003). Other felsic volcanic rocks are distributed along the IBA and in the back-arc seamount chains (Ishizuka et al., 1998; Hochstaedter et al., 2000, 2001). This representative distribution of rock types indicates that the lithology of the Nankai Trough is linked to the different geological units, which infers that the rock geochemistry can be used to reveal the subduction effects of different units.

The geochemical composition of rocks near the Nankai Trough shows that they are dominated by sub-alkaline series (Fig. 5a). The KPR rocks are dominated by basalt and basaltic andesite, indicating a typical oceanic basement (Fig. 5a). The KSC rocks are dominated by basalt and include a small amount of alkaline trachybasalt (Fig. 5a). The rock type of the IBA is complex, including a series of mafic-felsic volcanic rocks such as basalt, basaltic andesite, andesite, dacite, and rhyolite (Fig. 5a). In the FeO*/MgO versus SiO_2 diagram (FeO* represents total iron) (Fig. 5b), most of the volcanic rocks of this study belong to the tholeiitic series (TH), i.e., enriched in Fe compared with the calc-alkaline series (CA). The proportion of CA and TH can reflect depletion of the upper mantle, as magma produced by a depleted mantle has lower FeO*/MgO so tends to exhibit calc-alkaline characteristic (Miyashiro, 1974). Additional, in subduction-related environments, melting of a depleted mantle occurs under hydrous and oxidizing condition, which can promote magnetite crystallization and suppress plagioclase crystallization during magmatic evolution, leading to calc-alkaline magma with low FeO*/MgO (Danyushevsky, 2001; Berndt et al., 2005). The studied rocks

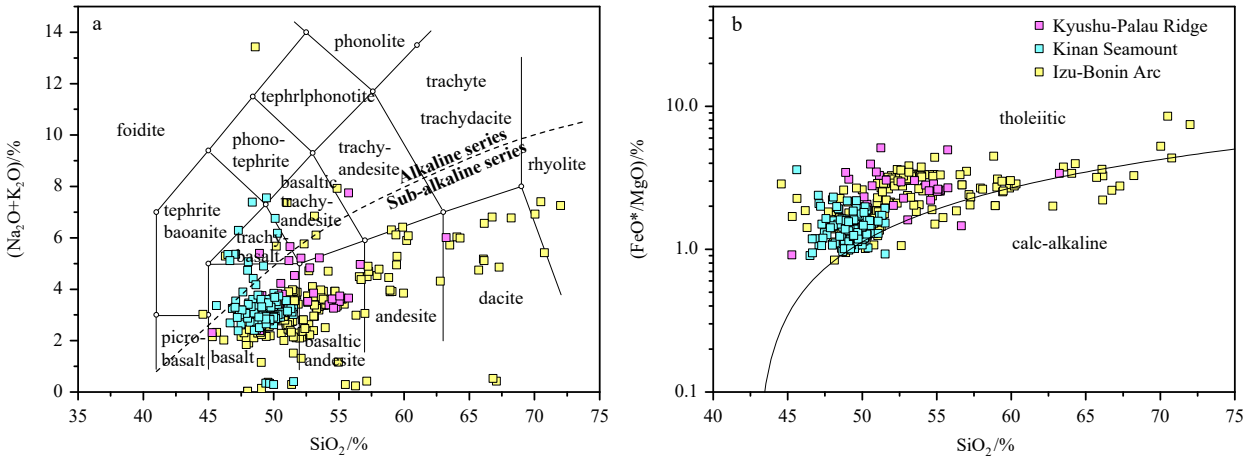

Fig. 5. SiO_2 vs. Na_2O+K_2O diagram (a) and SiO_2 vs. FeO*/MgO diagram (b) of rocks collected near the Nankai Trough (130°–139°E). FeO* represents the total iron. Rock data are derived from Ishizuka et al. (2003, 2009), Fukuda et al. (2008), Haraguchi et al. (2012), and the PetDB database (http://www.earthchem.org/petdb).

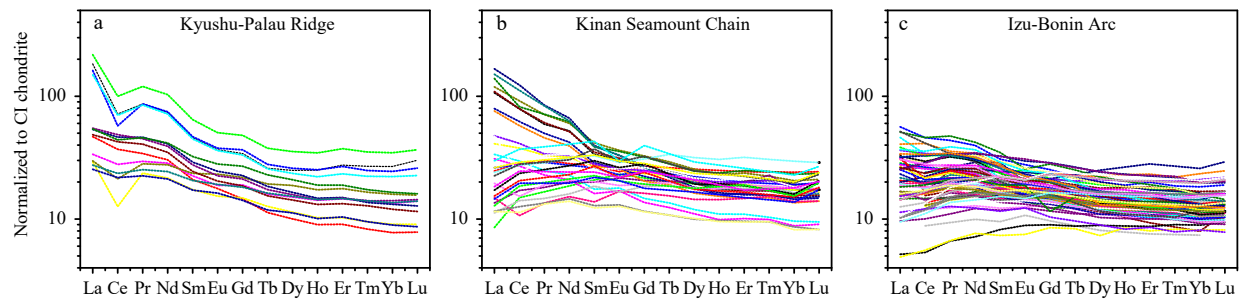

Fig. 6. Chondrite-normalized rare earth element diagram of basalt near the Nankai Trough (130°–139°E). Chondrite composition data are from Anders and Grevesse (1989). Rock data are derived from Hochstaedter et al. (2001), Ishizuka et al. (2003, 2009), Fukuda et al. (2008), Haraguchi et al. (2012), Freymuth et al. (2016), and the PetDB database (http://www.earthchem.org/petdb).

show an increasing proportion of CA for KPR, KSC, and IBA, which may indicate a progressively depleted mantle composition from west to east along the Nankai Trough.

The CI-normalized REE patterns of basalt are shown in Fig. 6. All basalts from the KPR have LREE-enriched patterns and the LREE contents are higher in basalts from the KPR and KSC than in basalts from the IBA. In addition, the proportions of LREE-enriched basalts in the KSC and IBA are significantly less than those of the KPR (Fig. 6). Although the REE pattern may be affected by mantle metasomatism events, the enrichment or depletion trend of REE is consistent with variations in the proportion of calc-alkaline lava. Therefore, the composition of lava may partly reflect the level of enrichment or depletion of the mantle source. The volcanic rocks from the northern part of the KPR are thought to have originated from an enriched mantle source (Haraguchi et al., 2012), whereas the basalts from the KSC are proposed to have been generated from a mantle source mixed by MORB-type and OIB-type mantle materials (Sato et al., 2002). These characteristics indicate that the composition of mantle underlying the different geological units may vary significantly; indeed, the mantle composition shows a gradually depleting trend from west to east along the Nankai Trough. The subduction effect of the compositional variation is discussed in Section 5.

Age-dating results indicate that most of the magmatic activity in the northern part of the IBA occurred from 0 Ma to 15 Ma and that the arc is still active nowadays (Fig. 7a). Tonalitic plutonic rocks dredged from the Komahashi-Daini Seamount in the northern KPR have K-Ar ages of ~38 Ma (Haraguchi et al., 2003). These tonalitic rocks record magmatic activity before the separation of the KPR from the proto-IBA arc due to opening of the Shikoku Basin (15–26 Ma). Volcanic rocks of the KSC are younger than 22 Ma and most have $^{40}Ar/^{39}Ar$ ages ranging from 15.7 Ma to 9.6 Ma (Ishizuka et al., 2009), whereas the age of the Shikoku Basin is 26–15 Ma (Okino et al., 1994, 1999). This indicates that volcanism was active after spreading of the Shikoku Basin (Fig. 7a). Post-spreading magmatism is consistent with the occurrence of the low-velocity mantle in the Shikoku Basin (Nakamura and Shibutani, 1998). The presence of high-temperature or partially melted asthenosphere would have increased volcanic activity in the Shikoku Basin after the spreading ceased, which is very common for marginal basins of the West Pacific (Sato et al., 2002). Young volcanic activity in the Shikoku Basin led to a hot subduction slab beneath the Nankai Trough, the subduction effect of which is discussed in Section 5.

The Pb isotope results of basalts (Fig. 7b) indicate that the IBA basalts have higher radioactive Pb isotopes than the KSC basalts, which is consistent with the origin of KPR from a proto-IBA that might have been affected by the addition of subduction components (dehydration fluids and sediment melt) to the mantle source of the arc basalts (e.g., Hochstaedter et al., 2001). In general, the basalts of the IBA, KSC, and KPR have higher $^{208}Pb/^{204}Pb$ ratios than those of Pacific basalts and are more likely to resemble the characteristics of Indian Ocean mantle (Fig. 7b). This is consistent with the composition of lavas from the PSP, which shows the typical characteristics of Indian Ocean-type MORB (Hickey-Vargas, 1991, 1998). Volcanic rocks from the overriding Japan Arc have higher $^{208}Pb/^{204}Pb$ ratios than rocks from the subduction PSP (Shibata et al., 2014), which may be related to the addition of highly radioactive Pb materials to the magma source due to melting of the subduction slab.

5 Discussion

5.1 *Current subduction stage of the KPR*

There are two notable differences between the subduction and collision models, i.e., the boundary and the vergence system (Tang et al., 2011; Beaumont et al., 1996). Firstly, a distinct boundary is observed between the subducting plate and the arc, whereas the boundary of the collision model (transition from subduction to collision) is not clear (Fig. 8). A low-gravity anomaly zone is observed at the transition zone from the PSP to the Nankai Trough (Fig. 2a). Tang et al. (2011) indicated that this feature was a boundary effect and proposed that the Nankai Trough acted as the boundary between the subducted PSP and the Japan Arc. Furthermore, the Nankai Trough is also easily identified in the bathymetric map, which exhibits a lower water depth than the surrounding areas (Figs 1 and 8). The existence of the clear boundary is consistent with the characteristics of the subduction model proposed by Beaumont et al. (1996). Secondly, the subduction model has primarily single vergence, whereas the collision (transition from subduction to collision) model exhibits double vergence (Fig. 8). Figure 8 shows that the subduction of

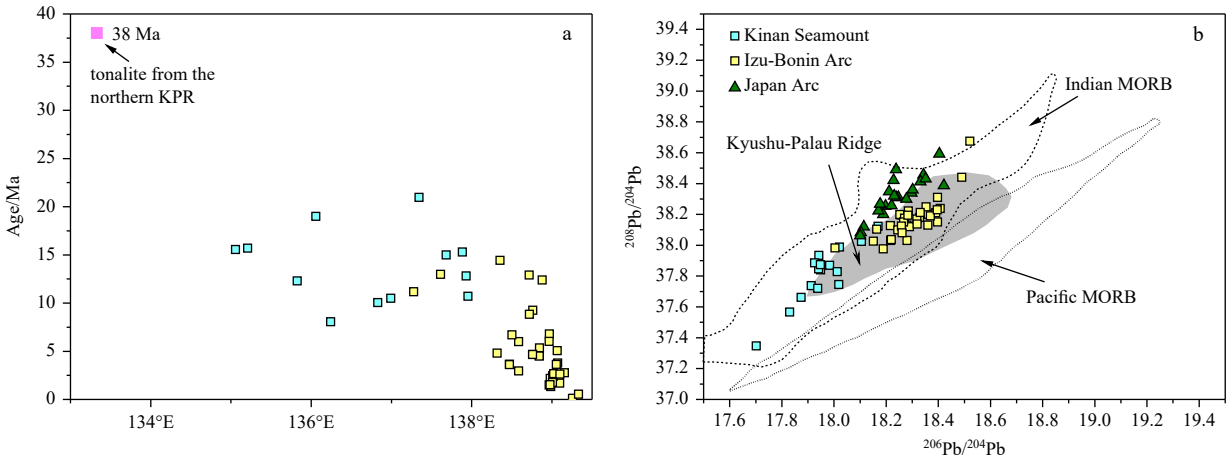

Fig. 7. Age of volcanic rock near the Nankai Trough (a) and Pb isotopes of volcanic rock from the Japan Arc (Shibata et al., 2014) and basalt near the Nankai Trough (130°–139°E) (b). Age data for tonalites are derived from Haraguchi et al. (2003). The Pb isotopes fields are derived from Yan and Shi (2011) and other data are derived from Ishizuka et al. (1998, 2009), Hochstaedter et al. (2001), and the PetDB database (http://www.earthchem.org/petdb).

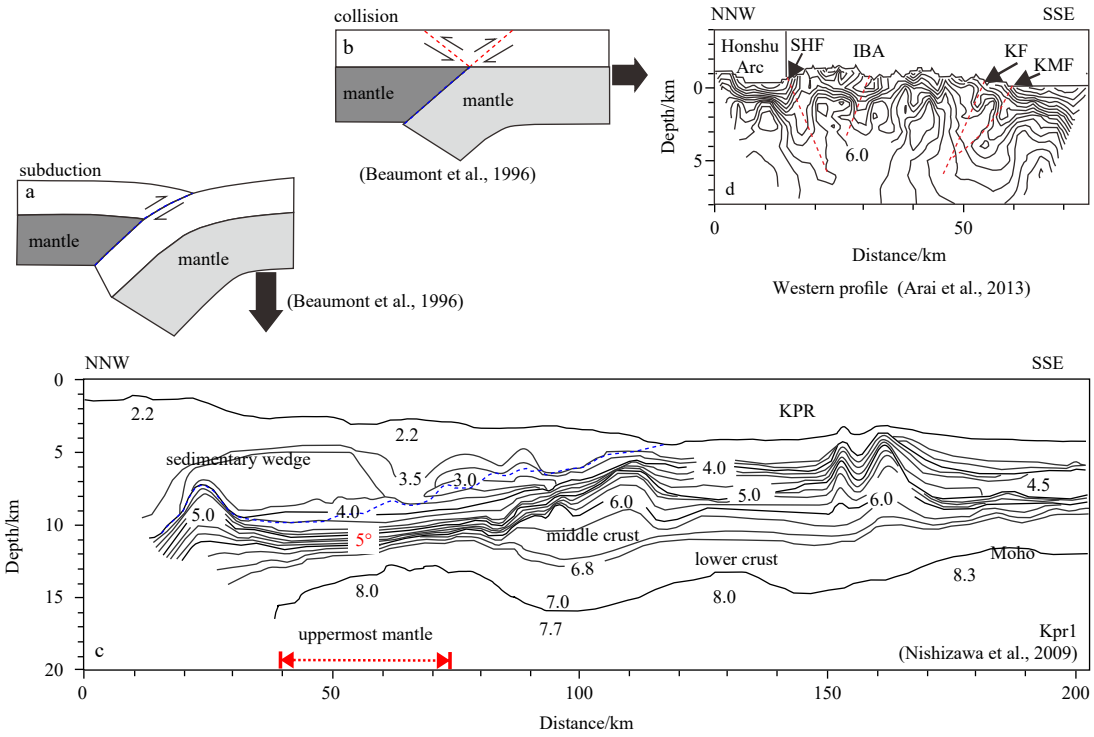

Fig. 8. Schematic diagram representing end member subduction (a) and collision (b) modified from Beaumont et al. (1996). Velocity structures of the KPR (c) and the IBA (d) modified from Nishizawa et al. (2009) and Arai et al. (2013), respectively. KPR: Kyushu-Palau Ridge, IBA: Izu-Bonin Arc.

KPR exhibits a single-vergence system, which differs from that of the IBA (double vergence characterized by inward-dipping thrust faults on both sides). All of these features indicate that the subducting KPR is in a subduction stage with no collision characteristics.

The geochemical characteristics also suggest that the KPR is still in the subducting stage and not an arc-arc collision stage. Collision between the IBA and the Honshu Arc resulted in the formation of granitoid plutons in the Izu collision zone of central Japan. These plutonic rocks represent continental crust material related to lateral accretion of Honshu Arc (Saito et al., 2007, 2012; Saito and Tani, 2017). Arc-arc collision resulted in transition from subduction of the IBA to accretion of IBA crust onto continental crust (Soh et al., 1998). The formation of felsic tonalite (Haraguchi et al., 2003) and a thick crust with a granitic material layer (Li et al., 1997) in the northern KPR may be related to continental crust accretion (Haraguchi et al., 2003). However, the tonalite have radiometric ages of ~38 Ma (Fig. 7a), indicating that felsic plutonic activity occurred during the early stages of arc volcanism before rifting of the IBA (Haraguchi et al., 2003). Therefore, the felsic tonalite and granitic crust layer may be related to vertical accretion of the continental crust instead of the arc-continent lateral accretion that occurs in the Izu collision zone (Saito et al., 2012; Saito and Tani, 2017). These results indicate that, instead of being attached to the Kyushu Arc, the KPR is being subducted underneath the Kyushu Arc at the Nankai Trough.

5.2 *Effect of aseismic ridge (seamount chain) subduction*

5.2.1 *Forearc deformation and angle of subduction*

A series of irregular concave topography is observed along the Nankai Trough subduction zone, which corresponds to the direction of the subducting KPR, KSC, and Zenisu Ridge (Figs 1 and 9). Figure 9 shows that the topographic features of the subducting KSC and Zenisu Ridge are consistent with the simulation results of seamount subduction (e.g., Dominguez et al., 2010). However, there is a spatial dislocation between the concave topography and the subducting KPR (Fig. 9). The KPR is considered to be a complex of closely spaced isolated seamounts (e.g., Tang et al., 2011) that subducts obliquely at the Nankai Trough (Tabei et al., 2003). Therefore, this displacement of topography is possibly caused by the oblique subduction of multiple seamounts. Therefore, we propose that the irregular concave topography of the Nankai Trough is due to aseismic ridge (seamount chain) subduction, and that closely spaced seamounts might explain the observed displacement of the concave shape.

Aseismic ridge (seamount chain) subduction along the subduction zone may also cause deformation of the overriding plate (Fig. 10) (e.g., Pautot and Rangin, 1989; Dominguez et al., 2000) and may be a mechanism for abrasion and erosion of the base of the overriding plate (Bangs et al., 2006). Park et al. (2009) analyzed a multi-channel seismic profile (KR0114-8) parallel to the Nankai Trough (near the KPR) and found an oceanic basement high on the subducting PSP between shot points 2400 and 3850 (Fig. 10). Three irregular peaks around shot points 2450, 3050, and 3650 were observed at the oceanic basement high, which approximately correspond to the topographic highs. Profile Ms104 (Fig. 10) also recorded the subducting KSC, which is 1.5 km higher than the oceanic crust (~28 km at Profile Ms104) (Park et al., 2009) and concordant with a basement high. These features indicate that aseismic ridge (seamount chain) subduction uplifts the overriding plate.

The subduction angle is primarily controlled by the age of the subducting slab (Peacock et al., 1994; Gutscher et al., 2000). To

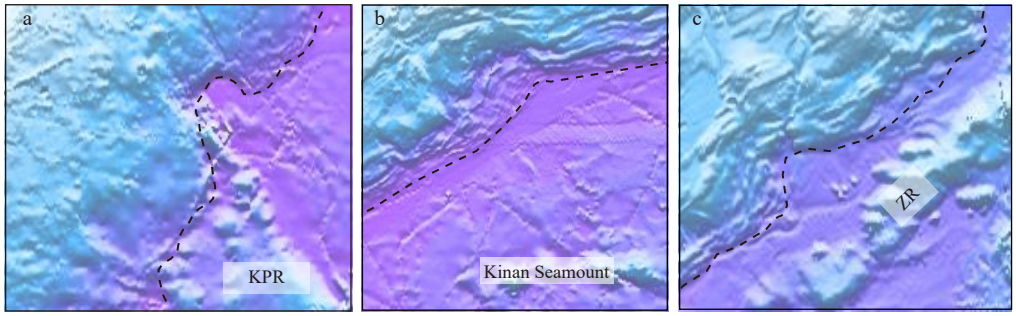

Fig. 9. Topographic map of the local area in the Nankai Trough. The black dotted line represents the deformation front. The positions of a, b, and c are shown in the white dotted box of Fig. 1. KPR: Kyushu-Palau Ridge, ZR: Zenisu Ridge.

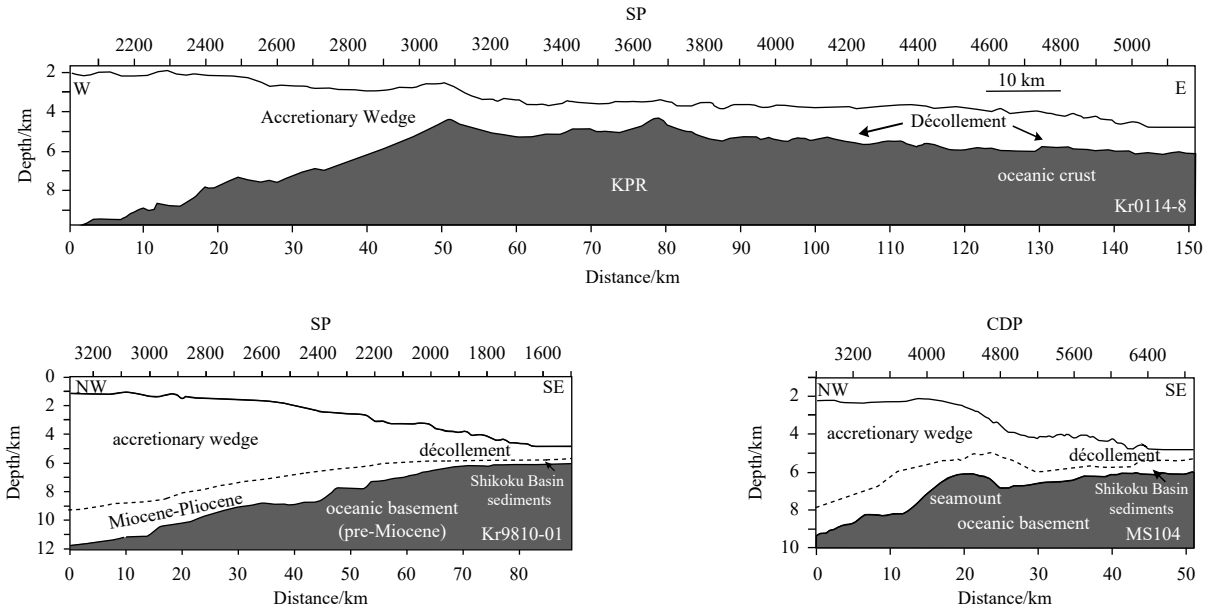

Fig. 10. Tectonic interpretation diagram of the multi-channel seismic profiles across or near the Nankai Trough (modified after Park et al. (2002, 2009)). KPR: Kyushu-Palau Ridge, SP: shot point, CDP: common depth point.

the west of the KPR, the older, colder, and denser West Philippine Basin lithosphere subducted steeply (Lallemand et al., 2005). To the east of the KPR, subduction of the younger, hotter, and lighter Shikoku Basin exhibited a gentler slab dip angle (Cao et al., 2014). This difference can be inferred by the depth contours of the upper surface of the subducted PSP in Fig. 1 (Nakajima and Hasegawa, 2007; Zhao et al., 2012), which suggests a relatively flat slab corresponding to subduction of the Shikoku Basin (Gutscher et al., 2000). The geochemical characteristics of this study indicate that the mantle composition beneath the KSC and IBA is more depleted than that of the KPR (Figs 5 and 6). Due to the loss of Fe and Al, the density of the depleted mantle is reduced (Niu et al., 2003), which may reduce the subduction angle of the slab. This is consistent with the gentler slab dip angle to the east of the KPR (Fig. 1). However, the subduction angle of the slab beneath the IBA is very steep, which is inconsistent with the depleted mantle composition. This may be because the oldest age of the IBA basement can be up to 49 Ma (Ishizuka et al., 2018); thus, the subduction angle is predominantly controlled by the old and cold nature of the subducting plate.

5.2.2 *Seismotectonics*

In addition to its importance to forearc deformation, aseismic ridge (seamount chain) subduction appears to be related to seismotectonics. The discussion here is predominantly based on three recent mega-earthquakes (the 1968 M_w 7.5 earthquake, the 1944 M_w 8.1 earthquake, and the 1946 M_w 8.3 earthquake) (Fig. 1) (Yagi et al., 1998; Kodaira et al., 2002; Park et al., 2009; Yamamoto et al., 2013). Liu and Zhao (2014) proposed that these mega-earthquakes occurred in or around strongly coupled areas, some of which might be produced by the KPR (the 1968 M_w 7.5 earthquake) and plutons intruded into the Kii Peninsula (the 1944 M_w 8.1 earthquake and the 1946 M_w 8.3 earthquake). Park et al. (2009) interpreted that a lack of mega-earthquakes at the western Kyushu section was due to the subducting KPR. As mentioned above, the flank regions of the subducting KPR are more likely to tear and result in slab fracturing, forming slab windows that may have acted as a barrier to rupture propagation of the Hyuga earthquake in 1968 (Park et al., 2009; Mason et al., 2010). In addition to slab fracturing, tectonic erosion of the base of the accretionary wedge caused by ridge (seamount chain) subduction may temporarily inhibit earthquake rupture by enhancing the fault-zone fluid content and reducing the fault-zone effective stress (Bangs et al., 2006). Kodaira et al. (2005) suggested that the strong coupling of the subducting paleo-Zenisu Ridge hindered the westward (Tokai offshore) extension of the Tonankai earth-

quake in 1944. The above characteristics are reflected in the rupture distributions of the 1969 and 1944 earthquakes (Figs 1 and 3). Kodaira et al. (2002) proposed that the subducting KSC also served as a barrier for the earthquake in 1946, which resulted in a short rupture that only extended to the locked zone in the east of the subducting seamount (Fig. 1). Moreover, the co-seismic rupture zone of the earthquake in 1946 was narrower the closer it was to the Kinan Seamount (Figs 1 and 3). In summary, the subducted aseismic ridge (seamount chain) along the Nankai Trough in recent mega-earthquakes (M_w> 8) might have served predominantly as a seismic barrier inhibiting rupture propagation.

5.2.3 *Magmatic activity*

Cao et al. (2014) imaged the 3D velocity structure beneath southwestern Japan using P-wave arrivals from local earthquakes and teleseismic events, and found that a high-velocity anomaly beneath the Abu volcano might be related to the subducted PSP; however, the anomaly was not continuous and instead interpreted as a low-velocity anomaly zone. This low-velocity anomaly was proposed to have been caused by the slab window. Previous studies show that the subduction direction of the PSP changed from NNW to NW at 2 Ma (Matsuda, 1980; Nakamura et al., 1984; Okamura, 1988), which led to variations in rollback rates and slab dip angles on both sides of the KPR. Therefore, some segments on the flank of the KPR could be fragile enough to spread laterally and split along the subducting ridge into the deep mantle (Mason et al., 2010). When the slab window extended into the deep mantle with the subducting KPR, hot mantle material rose through the slab window, leading to partial melting of the lower layers of the overriding plate (Mason et al., 2010) and the edge of the torn subducting plate (Yogodzinski et al., 2001). These processes resulted in adakitic and dacitic activity beneath the Abu volcano in southwestern Japan (Kakubuchi et al., 2000). Hence, we suggest that the subducting KPR may result in magmatism near the Nankai Trough.

In addition, partial melting of the oceanic crust resulting from subduction of the KPR may produce magma that contributes to the formation of porphyry copper deposits in the Kyushu Arc (Cooke et al., 2005). As Cu and Au are moderately incompatible elements, their contents in the oceanic crust are much higher than in the mantle and the continental crust. Therefore, magma formed by partial melting of the oceanic crust has higher Cu and Au contents, which is favorable for the formation of porphyry copper and gold deposits (Sun et al., 2004; 2011). Low-sulfidation epithermal gold deposits (Hishikari, 1.25–0.66 Ma) and high-sulfidation gold deposits (Nansatsu, 5.0–3.5 Ma) in the Kyushu arc overlap spatially with the subducted KPR (Fig. 1) (Cooke et al., 2005; Sun et al., 2010), which may be related to subduction of the KPR, leading to partial melting of the oceanic crust and enrichment of Cu and Au in the magma.

The ages of the volcanic rocks suggest that the subduction PSP is characterized by young volcanic activity (Fig. 7a). Subduction of the hot and young Shikoku Basin may lead to melting of the leading edge of the slab, which provided magma for Quaternary volcanoes (Daisen, Sambe, and Aonoyama) in Southwest Japan (Fig. 1) (Morris, 1995; Shibata et al., 2014). The andesite and dacite erupted in these volcanoes are chemically similar to adakites, which is consistent with their derivation by partial melting of the subducted slab (Morris, 1995; Shibata et al., 2014). These adakitic lavas have high radioactive Pb isotopes, which are related to melting of the subduction crust with an Indian Ocean-type MORB isotopic signature (Fig. 7b) (Hickey-Vargas, 1991, 1998). Therefore, both subduction of the KPR and the young Shikoku Basin play an important role in controlling the magmatic activity of the overriding plate.

6 Conclusions

The following conclusions can be drawn from this study:

(1) Gravity anomalies at the Nankai Trough vary significantly from the Philippine Sea Plate to the Japan Arc, with values concentrated in the range of –20 mGal to –40 mGal. Heat flow is high (60–200 mW/m²) in the middle part of the Nankai Trough and low (20–80 mW/m²) in western and eastern parts. The mantle composition is progressively depleted from west to east along the Nankai Trough. Four primary geological units identified as the Kyusyu-Palau Ridge, the Shikoku Basin, the Kinan Seamount Chain, and the Zenisu Ridge are subducting at the Nankai Trough, but with different velocity and density characteristics.

(2) The existence of the Nankai Trough indicates a distinct natural boundary between the subducting KPR and the Kyushu Arc. A single-vergence system was identified from the velocity structure for the subducting KPR, exhibiting different characteristics from that of the IBA (double-vergence system). Plutonic tonalites from the northern KPR may represent continental crust material but their radiometric age of ~38 Ma suggests that they are related to volcanism prior to rifting of the IBA instead of arc-continent accretion processes. All of these features indicate that the subducting KPR is still at the subduction stage, with no collision characteristics.

(3) Subduction of aseismic ridges (seamount chains) is a common process that occurs in a variety of tectonic settings, which may affect topography, structure, dynamics, and magmatism at or near the subduction zone. The overriding plate may have been deformed during subduction of the aseismic ridge (seamount chain), leading to an irregular concave topography along the front edge of the accretionary wedge. Aseismic ridge (seamount chain) subduction may have provided a seismic barrier inhibiting rupture propagation during the 1944 M_w 8.1 and 1946 M_w 8.3 earthquakes. Subduction of the KPR and hot, young Shikoku Basin lithosphere may have induced slab melting that resulted in adakitic magmatism and provided ore-forming metals for the formation of porphyry copper and gold deposits in the overriding Japan Arc.

Acknowledgements

We thank Yong Tang from the Second Institute of Oceanography, Ministry of Natural Resources and Quanshu Yan from the First Institute of Oceanography, Ministry of Natural Resources for their constructive suggestions. Most of the figures were plotted using GMT (Wessel and Smith, 1995).

References

Anders E, Grevesse N. 1989. Abundances of the elements: Meteoritic and solar. Geochimica et Cosmochimica Acta, 53(1): 197–214, doi: 10.1016/0016-7037(89)90286-x

Arai R, Iwasaki T, Sato H, et al. 2013. Crustal structure of the Izu collision zone in central Japan from seismic refraction data. Journal of Geophysical Research: Solid Earth, 118(12): 6258–6268, doi: 10.1002/2013JB010532

Bangs N L B, Gulick S P S, Shipley T H. 2006. Seamount subduction erosion in the nankai trough and its potential impact on the seismogenic zone. Geology, 34(8): 701–704, doi: 10.1130/G22451.1

Beaumont C, Ellis S, Hamilton J, et al. 1996. Mechanical model for subduction-collision tectonics of Alpine-type compressional orogens. Geology, 24(8): 675–678, doi: 10.1130/0091-7613(1996)024

<0675:MMFSCT>2.3.CO;2

Berndt J, Koepke J, Holtz F. 2005. An experimental investigation of the influence of water and oxygen fugacity on differentiation of MORB at 200 MPa. Journal of Petrology, 46(1): 135–167, doi: 10.1093/petrology/egh066

Cao Lingmin, Wang Zhi, Wu Shiguo, et al. 2014. A new model of slab tear of the subducting Philippine Sea Plate associated with Kyushu–Palau Ridge subduction. Tectonophysics, 636: 158–169, doi: 10.1016/j.tecto.2014.08.012

Chen Ping, Zheng Yanpeng, Liu Baohua. 2014. Geophysical features of the Nankai Trough subduction zone and their dynamic significance. Marine Geology & Quaternary Geology (in Chinese), 34(6): 153–160

Cooke D R, Hollings P, Walshe J L. 2005. Giant porphyry deposits: characteristics, distribution, and tectonic controls. Economic Geology, 100(5): 801–818, doi: 10.2113/gsecongeo.100.5.801

Cosca M, Arculus R, Pearce J, et al. 1998. $^{40}Ar/^{39}Ar$ and K–Ar geochronological age constraints for the inception and early evolution of the Izu–Bonin–Mariana arc system. Island Arc, 7(3): 579–595, doi: 10.1111/j.1440-1738.1998.00211.x

Danyushevsky L V. 2001. The effect of small amounts of H_2O on crystallisation of mid-ocean ridge and backarc basin magmas. Journal of Volcanology and Geothermal Research, 110(3–4): 265–280, doi: 10.1016/S0377-0273(01)00213-X

Dominguez S, Malavieille J, Lallemand S E. 2000. Deformation of accretionary wedges in response to seamount subduction: Insights from sandbox experiments. Tectonics, 19(1): 182–196, doi: 10.1029/1999TC900055

Freymuth H, Ivko B, Gill J B, et al. 2016. Thorium isotope evidence for melting of the mafic oceanic crust beneath the Izu arc. Geochimica et Cosmochimica Acta, 186: 49–70, doi: 10.1016/j.gca.2016.04.034

Fukuda S, Nakai S I, Niihori K, et al. 2008. 238U-230Th radioactive disequilibrium in the northern Izu arc: (230Th/232Th) in the sub-arc mantle. Geochemical Journal, 42(6): 461–479, doi: 10.2343/geochemj.42.461

GEBCO Compilation Group. 2020. GEBCO 2020 Grid, doi: 10.5285/a29c5465-b138-234d-e053-6c86abc040b9

Gutscher M A, Maury R, Eissen J P, et al. 2000. Can slab melting be caused by flat subduction?. Geology, 28(6): 535–538, doi: 10.1130/0091-7613(2000)28<535:CSMBCB>2.0.CO;2

Haraguchi S, Ishii T, Kimura J I, et al. 2003. Formation of tonalite from basaltic magma at the Komahashi-Daini Seamount, northern Kyushu-Palau Ridge in the Philippine Sea, and growth of Izu-Ogasawara (Bonin)-Mariana arc crust. Contributions to Mineralogy and Petrology, 145(2): 151–168, doi: 10.1007/s00410-002-0433-y

Haraguchi S, Ishii T, Kimura J I, et al. 2012. The early Miocene (~25 Ma) volcanism in the northern Kyushu-Palau Ridge, enriched mantle source injection during rifting prior to the Shikoku backarc basin opening. Contributions to Mineralogy and Petrology, 163(3): 483–504, doi: 10.1007/s00410-011-0680-x

Heki K, Miyazaki S I. 2001. Plate convergence and long-term crustal deformation in central Japan. Geophysical Research Letters, 28(12): 2313–2316, doi: 10.1029/2000GL012537

Hickey-Vargas R. 1991. Isotope characteristics of submarine lavas from the Philippine Sea: implications for the origin of arc and basin magmas of the Philippine tectonic plate. Earth and Planetary Science Letters, 107(2): 290–304, doi: 10.1016/0012-821X(91)90077-U

Hickey-Vargas R. 1998. Origin of the Indian Ocean-type isotopic signature in basalts from Philippine sea plate spreading centers: an assessment of local versus large-scale processes. Journal of Geophysical Research: Solid Earth, 103(B9): 20963–20979, doi: 10.1029/98JB02052

Hochstaedter A, Gill J, Peters R, et al. 2001. Across-arc geochemical trends in the Izu-Bonin arc: Contributions from the subducting slab. Geochemistry, Geophysics, Geosystems, 2(7): 1019, doi: 10.1029/2000GC000105

Hochstaedter A G, Gill J B, Taylor B, et al. 2000. Across-arc geochemical trends in the Izu-Bonin arc: Constraints on source composition and mantle melting. Journal of Geophysical Research: Solid Earth, 105(B1): 495–512, doi: 10.1029/1999JB900125

Idini B, Rojas F, Ruiz S, et al. 2017. Ground motion prediction equations for the Chilean subduction zone. Bulletin of Earthquake Engineering, 15(5): 1853–1880, doi: 10.1007/s10518-016-0050-1

Ishizuka O, Hickey-Vargas R, Arculus R J, et al. 2018. Age of Izu–Bonin–Mariana arc basement. Earth and Planetary Science Letters, 481: 80–90, doi: 10.1016/j.epsl.2017.10.023

Ishizuka O, Taylor R N, Milton J A, et al. 2003. Fluid–mantle interaction in an intra-oceanic arc: Constraints from high-precision Pb isotopes. Earth and Planetary Science Letters, 211(3–4): 221–236, doi: 10.1016/S0012-821X(03)00201-2

Ishizuka O, Uto K, Yuasa M, et al. 1998. K-Ar ages from seamount chains in the back-arc region of the Izu–Ogasawara arc. Island Arc, 7(3): 408–421, doi: 10.1111/j.1440-1738.1998.00199.x

Ishizuka O, Taylor R N, Yuasa M, et al. 2011. Making and breaking an island arc: A new perspective from the oligocene Kyushu-Palau Arc, Philippine sea. Geochemistry, Geophysics, Geosystems, 12(5): Q05005, doi: 10.1029/2010GC003440

Ishizuka O, Yuasa M, Taylor R N, et al. 2009. Two contrasting magmatic types coexist after the cessation of back-arc spreading. Chemical Geology, 266(3–4): 274–296, doi: 10.1016/j.chemgeo.2009.06.014

Kakubuchi S, Nagao T, Nagao K. 2000. K-Ar ages and magmatic history of the Abu Monogenetic Volcano Group, southwest Japan. Japanese Magazine of Mineralogical and Petrological Sciences, 29(5): 191–198, doi: 10.2465/gkk.29.191

Kimura J I, Kent A J R, Rowe M C, et al. 2010. Origin of cross-chain geochemical variation in Quaternary lavas from the northern Izu arc: Using a quantitative mass balance approach to identify mantle sources and mantle wedge processes. Geochemistry, Geophysics, Geosystems, 11(10): Q10011, doi: 10.1029/2010GC003050

Kobayashi K, Kasuga S, Okino K. 1995. Shikoku basin and its margins, In: Taylor B, ed. Backarc Basins. Boston, MA: Springer, 381–405

Kodaira S, Iidaka T, Kato A, et al. 2004. High pore fluid pressure may cause silent slip in the Nankai trough. Science, 304(5675): 1295–1298, doi: 10.1126/science.1096535

Kodaira S, Iidaka T, Nakanishi A, et al. 2005. Onshore-offshore seismic transect from the eastern Nankai Trough to central Japan crossing a zone of the Tokai slow slip event. Earth, Planets and Space, 57(10): 943–959, doi: 10.1186/BF03351874

Kodaira S, Kurashimo E, Park J O, et al. 2002. Structural factors controlling the rupture process of a megathrust earthquake at the Nankai Trough seismogenic zone. Geophysical Journal International, 149(3): 815–835, doi: 10.1046/j.1365-246X.2002.01691.x

Kodaira S, Takahashi N, Park J O, et al. 2000. Western Nankai Trough seismogenic zone: Results from a wide-angle ocean bottom seismic survey. Journal of Geophysical Research: Solid Earth, 105(B3): 5887–5905, doi: 10.1029/1999JB900394

Lallemand S, Heuret A, Boutelier D. 2005. On the relationships between slab dip, back-arc stress, upper plate absolute motion, and crustal nature in subduction zones. Geochemistry, Geophysics, Geosystems, 6(9): Q09006

Lee W H K. 1964. International heat flow committee. Eos, Transactions American Geophysical Union, 45(3): 441–444, doi: 10.1029/TR045i003p00441

Li K. 1997. Crustal structure of north Kyushu-Palau Ridge by ocean bottom seismographic observation. Proceedings of Seismological Society of Japan, 2: 38

Liu X, Zhao D P. 2014. Structural control on the nucleation of megathrust earthquakes in the Nankai subduction zone. Geophysical Research Letters, 41(23): 8288–8293, doi: 10.1002/2014GL062002

Mason W G, Moresi L, Betts P G, et al. 2010. Three-dimensional numerical models of the influence of a buoyant oceanic plateau on subduction zones. Tectonophysics, 483(1–2): 71–79, doi: 10.1016/j.tecto.2009.08.021

Matsuda T. 1980. Traces of Izu Peninsula—its direction of movement during the recent several million years. Earth Monthly, 2: 164–168

Maus S, Barckhausen U, Berkenbosch H, et al. 2009. EMAG2: A 2–arc min resolution Earth Magnetic Anomaly Grid compiled from satellite, airborne, and marine magnetic measurements. Geochemistry, Geophysics, Geosystems, 10(8): Q08005, doi: 10.1029/2009GC002471

Miyashiro A. 1974. Volcanic rock series in island arcs and active continental margins. American Journal of Science, 274(4): 321–355, doi: 10.2475/ajs.274.4.321

Morris P A. 1995. Slab melting as an explanation of Quaternary volcanism and aseismicity in southwest Japan. Geology, 23(5): 395–398, doi: 10.1130/0091-7613(1995)023<0395:SMAAEO>2.3.CO;2

Nakajima J, Hasegawa A. 2007. Tomographic evidence for the mantle upwelling beneath southwestern Japan and its implications for arc magmatism. Earth and Planetary Science Letters, 254(1–2): 90–105, doi: 10.1016/j.epsl.2006.11.024

Nakamura Y, Shibutani T. 1998. Three-dimensional shear wave velocity structure in the upper mantle beneath the Philippine Sea region. Earth, Planets and Space, 50(11–12): 939–952, doi: 10.1186/BF03352189

Nakamura K, Shimazaki K, Yonekura N. 1984. Subduction, bending and education; present and Quaternary tectonics of the northern border of the Philippine Sea Plate. Bulletin de la Société Géologique de France, S7-XXVI(2): 221–243, doi: 10.2113/gssgfbull.S7-XXVI.2.221

Nakanishi A, Shiobara H, Hino R, et al. 1998. Detailed subduction structure across the eastern Nankai Trough obtained from ocean bottom seismographic profiles. Journal of Geophysical Research: Solid Earth, 103(B11): 27151–27168, doi: 10.1029/98JB02344

Nakanishi A, Takahashi N, Park J O, et al. 2002. Crustal structure across the coseismic rupture zone of the 1944 Tonankai earthquake, the central Nankai Trough seismogenic zone. Journal of Geophysical Research: Solid Earth, 107(B1): EPM 2-1–EPM 2-21, doi: 10.1029/2001JB000424

Nishizawa A, Kaneda K, Oikawa M. 2009. Seismic structure of the northern end of the Ryukyu Trench subduction zone, southeast of Kyushu, Japan. Earth, Planets and Space, 61(8): e37–e40, doi: 10.1186/BF03352942

Nishizawa A, Kaneda K, Oikawa M, et al. 2017. Variations in seismic velocity distribution along the Ryukyu (Nansei-Shoto) Trench subduction zone at the northwestern end of the Philippine Sea plate. Earth, Planets and Space, 69: 86, doi: 10.1186/s40623-017-0674-7

Niu Yaoling, O'Hara M J, Pearce J A. 2003. Initiation of subduction zones as a consequence of lateral compositional buoyancy contrast within the lithosphere: A petrological perspective. Journal of Petrology, 44(5): 851–866, doi: 10.1093/petrology/44.5.851

Niu Xiongwei, Zhao Dapeng, Isozaki Y, et al. 2020. Structural heterogeneity and megathrust earthquakes in Southwest Japan. Physics of the Earth and Planetary Interiors, 298: 106347, doi: 10.1016/j.pepi.2019.106347

Okamura Y. 1988. Subduction of seamount and paleosubduction direction of the Philippine Sea Plate. Earth Monthly, 10: 603–607

Okino K, Ohara Y, Kasuga S, et al. 1999. The Philippine Sea: New survey results reveal the structure and the history of the marginal basins. Geophysical Research Letters, 26(15): 2287–2290, doi: 10.1029/1999GL900537

Okino K, Shimakawa Y, Nagaoka S. 1994. Evolution of the Shikoku basin. Journal of Geomagnetism and Geoelectricity, 46(6): 463–479, doi: 10.5636/jgg.46.463

Park J O, Hori T, Kaneda Y. 2009. Seismotectonic implications of the Kyushu-Palau Ridge subducting beneath the westernmost Nankai forearc. Earth, Planets and Space, 61(8): 1013–1018, doi: 10.1186/BF03352951

Park J O, Tsuru T, Takahashi N, et al. 2002. A deep strong reflector in the Nankai accretionary wedge from multichannel seismic data: Implications for underplating and interseismic shear stress release. Journal of Geophysical Research: Solid Earth, 107(B4): ESE 3-1–ESE 3-16, doi: 10.1029/2001JB000262

Pautot G, Rangin C. 1989. Subduction of the South China Sea axial ridge below Luzon (Philippines). Earth and Planetary Science Letters, 92(1): 57–69, doi: 10.1016/0012-821X(89)90020-4

Peacock S M, Rushmer T, Thompson A B. 1994. Partial melting of subducting oceanic crust. Earth and Planetary Science Letters, 121(1–2): 227–244, doi: 10.1016/0012-821X(94)90042-6

Pusok A E, Kaus B J P, Popov A A. 2018. The effect of rheological approximations in 3-D numerical simulations of subduction and collision. Tectonophysics, 746: 296–311, doi: 10.1016/j.tecto.2018.04.017

Sagiya T, Thatcher W. 1999. Coseismic slip resolution along a plate boundary megathrust: The Nankai Trough, southwest Japan. Journal of Geophysical Research: Solid Earth, 104(B1): 1111–1129, doi: 10.1029/98JB02644

Saito S, Arima M, Nakajima T, et al. 2007. Formation of distinct granitic magma batches by partial melting of hybrid lower crust in the Izu arc collision zone, central Japan. Journal of Petrology, 48(9): 1761–1791, doi: 10.1093/petrology/egm037

Saito S, Arima M, Nakajima T, et al. 2012. Petrogenesis of the Kaikomagatake granitoid pluton in the Izu Collision Zone, central Japan: implications for transformation of juvenile oceanic arc into mature continental crust. Contributions to Mineralogy and Petrology, 163(4): 611–629, doi: 10.1007/s00410-011-0689-1

Saito S, Tani K. 2017. Transformation of juvenile Izu–Bonin–Mariana oceanic arc into mature continental crust: an example from the Neogene Izu collision zone granitoid plutons, Central Japan. Lithos, 277: 228–240, doi: 10.1016/j.lithos.2016.07.035

Sandwell D T, Müller R D, Smith W H F, et al. 2014. New global marine gravity model from cryosat-2 and jason-1 reveals buried tectonic structure. Science, 346(6205): 65–67, doi: 10.1126/science.1258213

Sandwell D T, Smith W H F. 2009. Global marine gravity from retracked Geosat and ERS-1 altimetry: Ridge segmentation versus spreading rate. Journal of Geophysical Research: Solid Earth, 114(B1): B01411, doi: 10.1029/2008JB006008

Sato H, Machida S, Kanayama S, et al. 2002. Geochemical and isotopic characteristics of the Kinan Seamount Chain in the Shikoku Basin. Geochemical Journal, 36(5): 519–526, doi: 10.2343/geochemj.36.519

Shibata T, Yoshikawa M, Ujike O, et al. 2014. Along-arc geochemical variations in Quaternary magmas of northern Kyushu Island, Japan. Geological Society, London, Special Publications, 385(1): 15–29, doi: 10.1144/SP385.13

Soh W, Nakayama K, Kimura T. 1998. Arc–arc collision in the Izu collision zone, central Japan, deduced from the Ashigara Basin and adjacent Tanzawa Mountains. Island Arc, 7(3): 330–341, doi: 10.1111/j.1440-1738.1998.00193.x

Sun Weidong, Arculus R J, Kamenetsky V S, et al. 2004. Release of gold-bearing fluids in convergent margin magmas prompted by magnetite crystallization. Nature, 431(7011): 975–978, doi: 10.1038/nature02972

Sun Weidong, Ling Mingxing, Yang Xiaoyong, et al. 2010. Ridge subduction and porphyry copper-gold mineralization: An overview. Science China Earth Sciences, 53(4): 475–484, doi: 10.1007/s11430-010-0024-0

Sun Weidong, Zhang Hong, Ling Mingxing, et al. 2011. The genetic association of adakites and Cu–Au ore deposits. International Geology Review, 53(5–6): 691–703, doi: 10.1080/00206814.2010.507362

Tabei T, Hashimoto M, Miyazaki S, et al. 2003. Present-day deformation across the southwest Japan arc: Oblique subduction of the Philippine Sea plate and lateral slip of the Nankai forearc. Earth, Planets and Space, 55(10): 643–647, doi: 10.1186/BF03352471

Takahashi N, Kodaira S, Nakanishi A, et al. 2002. Seismic structure of western end of the Nankai Trough seismogenic zone. Journal of Geophysical Research: Solid Earth, 107(B10): ESE 2-1–ESE 2-19, doi: 10.1029/2000JB000121

Talwani M, Worzel J L, Landisman M. 1959. Rapid gravity computations for two-dimensional bodies with application to the Mendocino submarine fracture zone. Journal of Geophysical Research, 64(1): 49–59, doi: 10.1029/JZ064i001p00049

Tang Yong, Li Mingbi, Li Jiabiao, et al. 2011. The geomorphological features and continuity of the Kyushu-Palau Ridge (KPR). Acta Oceanologica Sinica, 30(5): 114–124, doi: 10.1007/s13131-011-0136-1

Wessel P, Smith W H. 1995. New version of generic mapping tools released. Eos, Transactions of the American Geophysical Union, 76(33): 329, doi: 10.1029/95EO00198

Wu Song, Zheng Youye, Sun Xiang. 2016. Subduction metasomatism and collision-related metamorphic dehydration controls on the fertility of porphyry copper ore-forming high Sr/Y magma in Tibet. Ore Geology Reviews, 73: 83–103, doi: 10.1016/j.oregeorev.2015.10.023

Xu Jiren, Zhao Zhixin, Kono Y, et al. 2003. Regional characteristics of stress field and its dynamics in and around the Nankai Trough, Japan. Chinese Journal of Geophysics (in Chinese), 46(4): 488–494

Yagi Y, Kikuchi M, Yoshida S, et al. 1998. Source process of the Hyuga-nada earthquake of April 1, 1968 (M_W 7.5), and its relationship to the subsequent seismicity. Zisin, 51(1): 139–148, doi: 10.4294/zisin1948.51.1_139

Yamamoto Y, Obana K, Takahashi T, et al. 2013. Imaging of the subducted Kyushu-Palau Ridge in the Hyuga-nada region, western Nankai Trough subduction zone. Tectonophysics, 589: 90–102, doi: 10.1016/j.tecto.2012.12.028

Yan Quanshu, Shi Xuefa. 2011. Geological comparative studies of Japan arc system and Kyushu-Palau Arc. Acta Oceanologica Sinica, 30(4): 107–121, doi: 10.1007/s13131-011-0134-3

Yogodzinski G M, Lees J M, Churikova T G, et al. 2001. Geochemical evidence for the melting of subducting oceanic lithosphere at plate edges. Nature, 409(6819): 500–504, doi: 10.1038/35054039

Zang Shaoxian, Ning Jieyuan. 2002. Interaction between the Philippine Sea plate and the Eurasia plate and its influence on the tectonics of eastern Asia. Chinese Journal of Geophysics, 45(2): 184–194, doi: 10.1002/cjg2.231

Zhang Jie, Li Jiabiao, Ding Weiwei. 2012. Reviews of the study on crustal structure and evolution of the Kyushu-Palau Ridge. Advances in Marine Science (in Chinese), 30(4): 595–607

Zhao Dapeng, Yanada T, Hasegawa A, et al. 2012. Imaging the subducting slabs and mantle upwelling under the Japan Islands. Geophysical Journal International, 190(2): 816–828, doi: 10.1111/j.1365-246X.2012.05550.x